International Journal of Heat and Mass Transfer 149 (2020) 119111

Contents lists available at ScienceDirect

International Journal of Heat and Mass Transfer

journal homepage: www.elsevier.com/locate/hmt

A new method to identify the optimal temperature of latent-heat thermal-energy storage systems for power generation from waste heat

Martin T. White*, Abdulnaser I. Sayma

Department of Mechanical Engineering and Aeronautics, School of Mathematics, Computer Science and Engineering, City, University of London, Northampton Square, London, EC1V 0HB, United Kingdom

ARTICLE INFO

Article history:
Received 1 April 2019
Accepted 24 November 2019

Keywords:
Latent-heat thermal-energy storage
TES
Waste-heat recovery
WHR
Power generation
ORC

ABSTRACT

The integration of thermal-energy storage (TES) within waste-heat recovery power generation systems has the potential to improve energy-efficiency in many industrial processes with variable and/or intermittent waste-heat streams. The first objective of this paper is to present a novel model of these systems that can be used at an early design stage to provide fast and accurate estimates of performance. More specifically, the method can identify the optimal temperature of latent-heat TES systems for waste-heat recovery applications based only on the known heat-source and heat-sink conditions (*i.e.*, temperature, mass-flow rate and specific-heat capacity), and can assess both single-stage and cascaded systems. The model has been validated against optimal organic Rankine cycle systems identified from a thermodynamic cycle optimisation. The second objective is to identify the characteristics of optimal systems for different heat-source profiles. The results indicate that, for a given application, there exists an optimal temperature for the latent-heat TES system that depends primarily on the relative size of the heat sink. Moreover, it is found that, for a heat engine operating with TES, the power rating ranges between 25% and 60% of the corresponding power rating for an optimal heat engine, operating without TES, that adapts instantaneously to heat-source fluctuations, whilst the total energy production is reduced by between 45% and 85% respectively. Finally, a small deviation is observed between the results obtained for the different heat sources considered, which suggests that these findings can be extrapolated to other heat sources not considered within this study.

1. Introduction

It is well known that energy storage is a key enabling technology to achieve targeted future scenarios for renewable energy generation [1,2]. Whilst electrical-storage technologies remain a focus, thermal-energy storage (TES) technologies are important to match the availability of thermal energy with the demand for either direct heating, power generation or cooling [3,4]. Most developments in TES technologies can be linked to solar-thermal applications [5], such as domestic solar-thermal heating systems [6], and concentrated-solar power (CSP) plants [7]. The simplest of these systems, such as a domestic solar-thermal heating system, simply stores thermal energy in a hot-water tank, whilst large-scale CSP plants implement molten salts. However, TES power generation systems could have wider importance in any application where variable and/or intermittent heat sources are used to generate power. This includes a range of current and future power generation systems, including micro-gas turbines [8], organic Rankine cycles (ORC) [9] and supercritical CO_2 cycles [10].

Alongside implementing renewable technologies, it is critical to improve the energy efficiency of industrial processes. As such, energy-intensive industries, such as glass, iron and steel, cement, oil and gas and food and drink, are in the spotlight due to the large proportion of their total energy consumption that they reject to the environment in the form of waste heat [11–13]. Therefore, waste-heat recovery (WHR) technologies have an important role in improving energy efficiency and reducing the environmental impact of these industries. Of the options available, power generation appears to be one of the most promising options. The nature of the power generation unit depends on the temperature of the waste-heat stream, but will generally operate with steam, an organic fluid or even supercritical CO_2. It is worth noting that a large percentage of industrial waste heat is rejected at relatively low temperatures; for example, within the U.S. 90% of waste heat is available below 316 °C [11], whilst in China 54% is available at temperatures below 500 °C [14]. Therefore, ORC systems remain one of the most promising candidates, and one study estimates that the installation

* Corresponding author.
E-mail address: martin.white@city.ac.uk (M.T. White).

https://doi.org/10.1016/j.ijheatmasstransfer.2019.119111
0017-9310/

Nomenclature

HE	Heat engine
ORC	Organic Rankine cycle
PCM	Phase-change material
TES	Thermal-energy storage
WHR	Waste-heat recovery

Greek Symbols

η	Thermal efficiency
γ	Heat-capacity ratio, $(\dot{m}c_p)_c/(\dot{m}c_p)_h$
θ	TES temperature, $(T_{h,av} - T_{tes})/(T_{h,av} - T_{ci})$

Roman Symbols

ΔT_p	Heat exchanger pinch point, K
$\dot{m}$	Mass-flow rate, kg/s
$\dot{Q}$	Heat-transfer rate, J/s
$\dot{W}$	Power, J/s
PB	Payback period, years
SIC	Specific-investment cost, £/kW
C_0	Total cost of equipment, £
C_e	Cost of electricity, £/kWh
c_p	Specific-heat capacity, J/(kg K)
E	Total energy production, kWh
n	Operational hours, hours
P	Profit, £
Q	Thermal energy, J
T	Temperature, K
t	Time, s

Subscripts

0	Start
av	Average
c	Cold (heat sink)
ci	Cold inlet
co	Cold outlet
f	Final
h	Hot (heat source)
hi	Hot inlet
ho	Hot outlet
max	Maximum (comparable heat sink)
max,∞	maximum (infinite heat sink
tes	Thermal-energy storage

of ORC systems across 27 EU countries could generate 20 TWh of electricity a year [15].

However, one issue surrounding WHR is that many waste-heat sources are variable and intermittent in nature, varying in temperature, mass-flow rate and even composition of the fluid carrying the waste heat as a result of the production process. In this case, different strategies to mitigate the variability in the heat-recovery process exist, including: (i) sizing the power generation unit for a baseline thermal input that is less than the peak thermal power available; (ii) implementing a complex control strategy to control the power generation unit in line with the fluctuating heat source; and (iii) coupling the power generation unit to TES. The first option is incapable of fully exploiting all of the heat available, whilst option two would maximise energy production but would be associated with higher costs since it should be sized for the peak thermal power and would require a complex control strategy. Moreover, option two only provides power when heat is available as opposed to when required. Hence, the implementation of TES, which should allow a relatively high recovery of waste heat, whilst providing stable operating conditions for the power generation unit or the possibility of producing power on demand, represents a promising option.

To date there have been a few studies investigating coupled ORC and TES systems for solar power applications. Freeman et al. [16] compared sensible-heat storage and phase-change materials (PCM) for a domestic-scale combined heat and power system, and found that PCMs could increase energy production per unit volume of storage by up to 20%, whilst Rodríguez et al. [17] conducted a techno-economic assessment of a 1 MW CSP-ORC system operating with TES. In terms of WHR applications, Miró et al. [18] reviewed case studies in which TES has been applied, but do not focus explicitly on power generation. Bufi et al. [19] conducted a multi-objective optimisation of an ORC-TES system for WHR from an externally-fired gas turbine. The aim was to identify optimal cycles that represent the trade-off between thermal efficiency and heat-exchanger requirements. Lecompte et al. [20] studied WHR from an electric arc furnace, using an intermediate steam buffer or thermal oil loop to mitigate heat-source variability. Pantaleo et al. [21] compared an ORC-TES system to a micro-gas turbine for WHR within the coffee industry, and used a lumped-mass model to determine the optimal volume of a sensible-heat TES system. Dal Magro et al. [22] investigated retrofitting a PCM to an existing ORC system within the steel industry. The results suggest that the introduction of PCM could increase the capacity factor of the ORC system by between 38% and 52%, and the authors note the ability of the PCM to smooth the thermal inputs into the ORC. Finally, Jiménez-Arreola et al. [23] note the current lack of literature in the area of TES systems for WHR and attempt to provide an overview of the challenges. The authors stated that latent-heat TES system can provide a near constant thermal input into an ORC, thereby reducing off-design conditions, but have drawbacks such as increased exergy destruction due to the additional heat-transfer processes, and additional costs associated with increased complexity.

From these previous studies, latent-heat TES systems appear to have the potential to improve the performance of WHR power generation systems that utilise intermittent and variable heat streams. However, unlike solar applications, the optimal temperature of a latent-heat TES system for WHR is not clear. In solar applications, where the heat-transfer loop between the heat source and the TES material is a closed loop, it is advantageous to maintain the TES material at a temperature that is close to the heat-source temperature to maximise cycle thermal efficiency. However, in WHR applications the heat-source is available as an open stream [24], which means the melting temperature of the TES material has a direct effect on the amount of heat that can be recovered, as shown qualitatively in Fig. 1. If the TES temperature, T_{tes}, is low (Fig. 1a), the TES extracts a large amount of heat from the heat source, $\dot{Q}_h$. However, the low temperature difference between the TES and heat sink result in a low heat engine thermal efficiency, η (*i.e.*, $\eta \propto T_{tes}/T_c$). On the other hand, if the TES temperature is high (Fig. 1b), the heat extracted from the waste-heat stream is low, whilst the thermal efficiency is high. Therefore, since the power production is equal to the product of these two parameters (*i.e.*, $\dot{W} = \eta \dot{Q}_h$), an optimal value for T_{tes} must exist. It is worth noting that cascaded latent-heat TES systems, in which the TES system is comprised of multiple TES materials each with a different melting temperature, can improve the performance of latent-heat TES systems [25]. In this case it is necessary to optimise the temperature of each TES stage, as demonstrated in Ref [26]. However, these studies have predominantly focussed on solar applications.

In summary, existing studies concerning TES for WHR recovery have not investigated the trade-off depicted in Fig. 1 in detail, and only consider a single case study, and hence cannot be widely extrapolated to other applications. Hence, the objective of this paper is to conduct a systematic investigation of WHR power generation units, coupled to TES, to identify the optimal characteristics of the

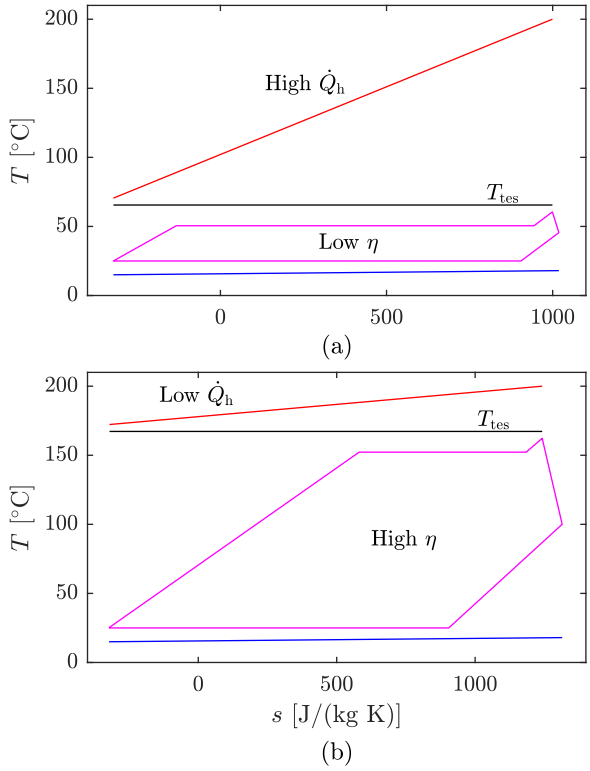

Fig. 1. Effect of the latent-heat storage temperature T_{tes} on the amount of heat extracted from the heat source $\dot{Q}_h$ and the efficiency of the heat engine η. Red, black, magenta and blue lines correspond to the heat source, TES, ORC, and heat sink respectively. (For interpretation of the references to colour in this figure legend, the reader is referred to the web version of this article.)

system, namely the optimal TES temperature. This is achieved by developing a novel model of the system that can quickly assess its performance for a particular heat source and heat sink. This facilitates a systematic investigation into the effect of the variability of the heat-source profile, the average heat-source temperature and the heat sink availability on the performance of the system to be completed. Thus, it is possible to define general design guidelines for these systems the can aid in the future development of these systems. Following this introduction, a description of the developed model is provided in Section 2. Then, in Section 3, this model is applied to two representative heat sources defined intentionally for this study, in addition to real waste-heat profiles taken from the literature. The conclusions from this study are summarised in Section 4.

2. Model of the system

2.1. Heat-engine model for a sensible-heat source

For this study, a model to predict the maximum power that can be produced from a defined heat source and heat sink is sought. This should predict the expected performance based on these inputs, without requiring more details on the heat engine, such as the cycle architecture, working fluid and cycle operating conditions. For this purpose finite-time thermodynamics can be applied. Within a Carnot heat engine the working fluid is at thermal equilibrium with the heat source and heat sink reservoirs, which implies infinitely long heat exchange processes that cannot be achieved in practice. In comparison, finite-time thermodynamics assumes that heat exchange processes are finite, which leads to an expression for the thermal efficiency that corresponds to the maximum work output from the cycle. This expression, referred to

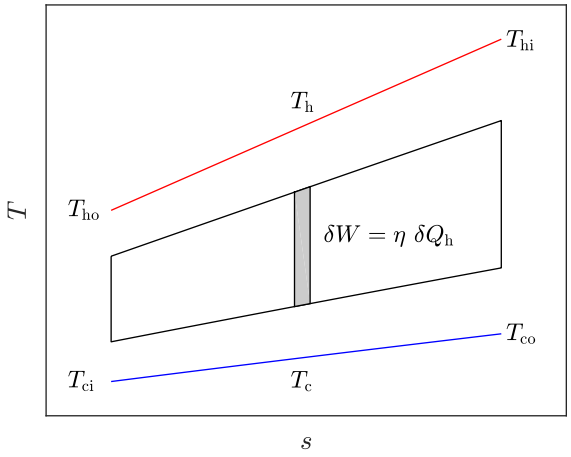

Fig. 2. Schematic of a theoretical heat engine operating with a sensible heat source represented on a $T - s$ plot.

as the Novikov [27] or Curzon-Ahlborn [28] efficiency, is defined as:

$$\eta = 1 - \sqrt{\frac{T_c}{T_h}}\,. \tag{1}$$

where T_c and T_h are the heat-sink and heat-source temperatures respectively, which are assumed constant.

The concept of finite-time thermodynamics has been the subject of further studies within the literature. Rubin [29,30] discussed that in practice there is often a trade-off between maximising thermal efficiency and maximising power, whilst Ondrechen et al. [31] and Wu [32] extended the analysis to consider heat reservoirs with finite heat capacities; both showed that these can have a large effect on thermodynamic performance. Furthermore, Ibrahim et al. [33] accounted for internal irreversibilities within the cycle; an idea that has also been explored by Chen [34] and Long and Liu [35]. Angulo-Brown [36] introduced the ecological criterion as an optimisation objective that targets a compromise between maximum power production and the minimum generation of entropy within the system. Overall, these studies demonstrate the potential of finite-time thermodynamics to assess heat engine performance without a detailed knowledge of the system. However, despite a few studies that compare these models to real thermodynamic cycles [37,38] and heat recovery processes [39], most studies are not related to physical systems. Moreover, the application of such models to TES systems has not been considered.

Within this work, a theoretical heat engine is considered that operates between a heat source and heat sink with defined inlet conditions (*i.e.*, temperature T, mass-flow rate $\dot{m}$ and specific-heat capacity c_p), as depicted in Fig. 2. The high-temperature and low-temperature heat-exchange processes are assumed to be counter-current, and experience a temperature reduction and increase respectively, whilst constant specific-heat capacities are assumed. The total power that can be produced for a given change in the heat-source temperature is given by:

$$\dot{W} = \int \eta\ \mathrm{d}\dot{Q}_h = (\dot{m}c_p)_h \int_{T_{ho}}^{T_{hi}} \eta\ \mathrm{d}T_h\,, \tag{2}$$

where $\dot{m}_h$ and $c_{p,h}$ are the mass-flow rate and specific-heat capacity of the heat source, η is the thermal efficiency of the heat engine, and T_{hi} and T_{ho} are the heat-source inlet and outlet temperatures respectively.

To integrate Eq. (2), an expression for the thermal efficiency η is required. One option is to use the Carnot efficiency ($\eta = 1 - T_c/T_h$). However, as stated previously, this assumes infinite heat exchange processes. Instead, the efficiency for a heat engine with finite

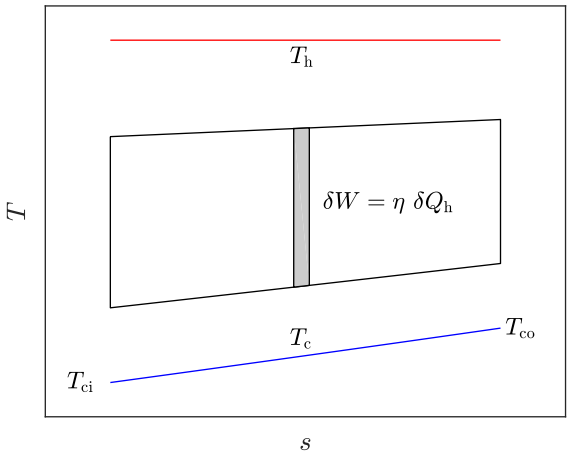

Fig. 3. Schematic of a theoretical heat engine operating with a latent heat source represented on a $T - s$ plot.

heat exchange processes will be applied (Eq. (1)). It is also noted from Fig. 2 that the heat-source and heat-sink temperatures vary throughout the heat-exchange processes. Applying an energy balance, the change in heat-sink temperature $\mathrm{d}T_\mathrm{c}$ can be calculated from:

$$\mathrm{d}T_\mathrm{c} = \left(\frac{1-\eta}{\gamma}\right)\mathrm{d}T_\mathrm{h}\,, \tag{3}$$

where γ is the heat-capacity ratio, $(\dot{m}c_p)_\mathrm{c}/(\dot{m}c_p)_\mathrm{h}$.

The solution to Eqs. (1)–(3) results in an estimate for the power output from a heat engine, based on the heat-source inlet and outlet temperatures, T_hi and T_ho, the heat-sink temperature T_ci and the heat-capacity ratio γ. Moreover, it follows that an optimal value for T_ho exists, which can be reasoned by considering two limiting cases when $\gamma = 1$. When $T_\mathrm{ho} = T_\mathrm{hi}$ no heat is extracted from the heat-source and hence $\dot{W} = 0$. On the other hand, when $T_\mathrm{ho} = T_\mathrm{ci}$, all of the heat extracted from the heat source is transferred to the heat sink, and hence $\dot{W} = 0$. Therefore, an optimum occurs at $\mathrm{d}\dot{W}/\mathrm{d}T_\mathrm{ho} = 0$, and this will occur between the limits $T_\mathrm{hi} > T_\mathrm{ho} > T_\mathrm{ci}$. Within this study, the solution to Eqs. (1)–(3) is completed numerically, and the golden ratio search is used to find the optimal value of T_ho.

2.2. Heat-engine model for a latent-heat source

For a latent-heat source, the solution is simpler since the heat source does not change temperature. A schematic of the theoretical latent-heat heat engine is shown in Fig. 3. For this system, the power output is given by the following:

$$\dot{W} = (\dot{m}c_p)_\mathrm{c}\int_{T_\mathrm{co}}^{T_\mathrm{ci}}\left(\frac{\eta}{1-\eta}\right)\mathrm{d}T_\mathrm{c}\,, \tag{4}$$

where all parameters have the same meaning as before, and η is defined by Eq. (1). Integrating Eq. (4), and assuming the heat engine extracts a certain amount of heat from the latent-heat store, $\dot{Q}_\mathrm{h}$, which is at a constant temperature T_h, the heat-sink outlet temperature is given by:

$$T_\mathrm{co} = \left(\frac{\dot{Q}_\mathrm{h}}{2\sqrt{T_\mathrm{h}}(\dot{m}c_p)_\mathrm{c}} + \sqrt{T_\mathrm{ci}}\right)^2. \tag{5}$$

Thus, the amount of heat rejected to the heat sink, $\dot{Q}_\mathrm{c} = (\dot{m}c_p)_\mathrm{c}(T_\mathrm{co} - T_\mathrm{ci})$, and power output from the heat engine, $\dot{W} = \dot{Q}_\mathrm{h} - \dot{Q}_\mathrm{c}$, can be obtained.

Ultimately, for a latent-heat source, $\dot{W}$ depends only on the available heat sink, and can be calculated based on the heat-sink inlet conditions, T_ci and $(\dot{m}c_p)_\mathrm{c}$, the latent-heat source temperature, T_h, and an assumed value for the heat extracted from the latent-heat source $\dot{Q}_\mathrm{h}$.

2.3. Latent-heat thermal-energy storage model

Within this work, the performance of a heat engine coupled to latent-heat TES (HE-TES) will be investigated for a time-varying heat-source. The heat-source is assumed to have a constant specific-capacity, whilst the mass-flow rate and temperature are functions of time, denoted $\dot{m}_\mathrm{h}(t)$ and $T_\mathrm{t}(t)$ respectively. To compare heat engines operating with and without latent-heat TES, the heat-engine model described in Section 2.1 is used to obtain the instantaneous power that could be obtained from the heat-source at a given time:

$$\dot{W}(t) = f(\dot{m}_\mathrm{h}(t),\ T_\mathrm{h}(t),\ c_{p,\mathrm{h}},\ T_\mathrm{ci},\ \gamma)\,. \tag{6}$$

The maximum energy that could be extracted, E_max, assuming that the heat engine adapts instantaneously to changes in the heat source can be obtained from:

$$E_\mathrm{max} = \int_{t_0}^{t_\mathrm{f}} \dot{W}(t)\ \mathrm{d}t\,, \tag{7}$$

where t_0 and t_f are the start and end times respectively.

For the HE-TES system, the amount of heat absorbed by the TES is given by:

$$Q_\mathrm{h} = \int_{t_0}^{t_\mathrm{f}} \dot{m}_\mathrm{h}(t)c_p[T_\mathrm{h}(t) - (T_\mathrm{tes} + \Delta T_\mathrm{p})]\ \mathrm{d}t\,, \tag{8}$$

where T_tes is the temperature of the thermal store, and ΔT_p is an assumed pinch point between the heat source and the TES at the exit of the TES system. In this analysis, it is assumed that the heat-transfer area between the heat source and TES material is sufficiently large such that T_ho is approximately equal to T_tes, with $\Delta T_\mathrm{p} = 2$ K.

When operating with TES, the heat engine, in principle, operates under a steady state. Therefore, assuming that during the complete operating cycle of the system, all the heat that is absorbed from the heat source is subsequently extracted from the TES by the heat engine, the heat-transfer rate into the heat engine is calculated from:

$$\dot{Q}_\mathrm{h} = \frac{Q_\mathrm{h}}{t_\mathrm{f} - t_0}\,, \tag{9}$$

from which $\dot{W}$ can be obtained using the model described in Section 2.2. The total energy produced is then:

$$E = \dot{W}(t_\mathrm{f} - t_0)\,. \tag{10}$$

The performance of the HE-TES system can then be evaluated by normalising the total energy production by the maximum energy that could have been theoretically produced (*i.e.*, E/E_max).

2.4. Cascaded latent-heat thermal-energy storage systems

The model for a single-stage HE-TES system can be extended to cascaded HE-TES systems, by connecting multiple versions of the single-stage model together, as illustrated in Fig. 4. In this case, the heat-source outlet conditions from the first stage feed into the second stage and so on for as many stages as required. From this, the total amount of heat absorbed by each stage, $Q_{\mathrm{h},i}$, can be calculated using Eq. (8), whilst the heat-transfer rate into the heat engine, $\dot{Q}_{\mathrm{h},i}$, can be calculated using Eq. (9). Then, starting at the last stage and working backwards, the heat-sink outlet temperature for each stage can be determined using Eq. (5). To identify the optimal temperature of each TES stage (denoted with the non-dimensional

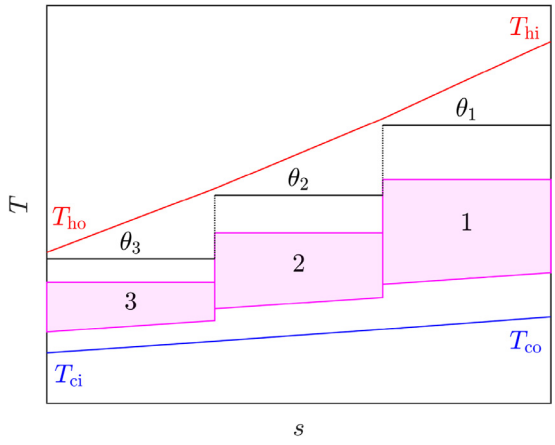

Fig. 4. Schematic of a theoretical heat engine operating with a cascaded latent-heat TES system.

form, $\theta_i = (T_{h,av} - T_{tes,i})/(T_{h,av} - T_{ci})$), an optimisation can be completed, which is expressed as:

$$\max \ \dot{W} = f(\mathbf{x}) \,, \tag{11}$$

where $\dot{W}$ is the total power generated by the complete system, and can be calculated from:

$$\dot{W} = \sum_{i=1}^{n} \dot{W}_i(\theta_i) \,, \tag{12}$$

and $\mathbf{x}$ is the vector of optimisation variables, denoted:

$$\mathbf{x} = [\theta_1, \quad \theta_2, \quad \theta_3, \quad \ldots \quad , \quad \theta_n], \tag{13}$$

where n is the number of stages.

2.5. Validation of heat-engine models

The suitability of Eq. (1) to predict the efficiency of real heat engines has been demonstrated previously [40]. However, this is based only on the inlet temperatures of the heat source and heat sink. To conduct a more thorough investigation within this work, the models have been validated by comparing results to optimal organic Rankine cycle (ORC) systems identified from a cycle optimisation study. For this, a subcritical recuperated ORC is considered and for a given working fluid the condensation temperature, evaporation pressure and expander inlet temperature are optimised to maximise the net power output from the cycle. The assumptions for the ORC system are listed in Table 1, whilst ORC cycle analysis is widely reported within the literature (see for example Ref. [41]) and will not be discussed here. For a sensible heat source, the heat-source temperature drop is introduced as an optimisation variable. For the conditions listed in Table 2 the ORC optimisation is completed for 31 different fluids and the fluid with the highest power output is compared to the power output predicted by the heat-engine model. The results for the sensible- and latent-heat systems are shown in Figs. 5 and 6.

For the sensible-heat systems (Fig. 5) it is observed that for $T_{hi} > 450$ K, and $(\dot{m}c_p)_c > 2.5$ kW/K, the difference in the power output from the ORC system and that predicted by the heat-engine model is less than 20%, relative to the heat-engine model. For lower heat-source temperatures a larger difference is observed, and at $T_{hi} = 373$ K the optimal ORC systems only produce 50% of the power predicted by the heat-engine model. This is attributed to these ORC systems having low pressure ratios, which results in most of the heat-transfer within the cycle occurring under isothermal conditions, resulting in significantly larger exergy destruction compared to the heat-engine model. Small heat-sink heat-capacity rates correspond to larger deviations since these are associated with a larger heat-sink temperature rise, which increases the ORC condensation temperature and hence also increases exergy destruction. The non-continuous nature of Fig. 5 is attributed to the

Table 1
Fixed parameters for the ORC optimisation study.

Pump isentropic efficiency, η_p	70	%
Expander isentropic efficiency, η_t	80	%
Recuperator effectiveness, ε_r	75	%
Heat-exchanger minimum pinch point	10	K

Table 2
Heat-source and heat-sink conditions considered for the validation study; $(\dot{m}c_p)_h$ applies only for the sensible-heat system and $\dot{Q}_h$ applies only for the latent-heat system.

T_{hi} [K]	T_{ci} [K]	$(\dot{m}c_p)_c$ [kW/K]	$(\dot{m}c_p)_h$ [kW/K]	$\dot{Q}_h$ [kW]
373–673	288	1, 2.5, 5, 10	1	100

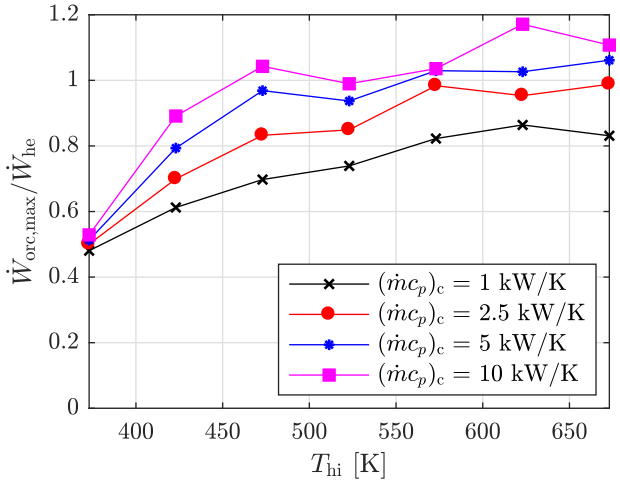

Fig. 5. Validation of the sensible-heat heat-engine model. For each heat-source temperature and heat-sink heat-capacity rate, the ORC with the highest power output $\dot{W}_{orc,max}$ is compared to the power output predicted by the sensible-heat heat-engine model $\dot{W}_{he}$.

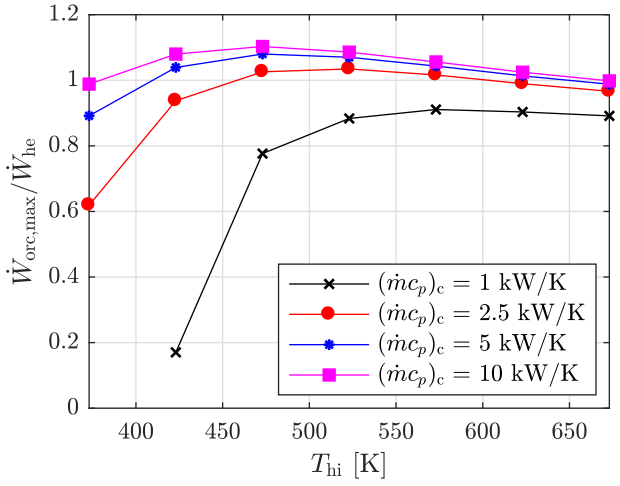

Fig. 6. Validation of the latent-heat heat-engine model. For each heat-source temperature and heat-sink heat-capacity rate, the ORC with the highest power output $\dot{W}_{orc,max}$ is compared to the power output predicted by the latent-heat heat-engine model $\dot{W}_{he}$.

Table 3
Sensitivity study on the effects of component performance on the power output from the ORC system. Results are given as a percentage deviation from the equivalent results obtained for $\eta_p = 0.7$, $\eta_t = 0.8$ and $\varepsilon_r = 0.75$. Standard deviation is given in the brackets.

	η_p		ε_r			η_t	
	0.5	0.9	0.0	0.5	1.0	0.7	0.9
Sensible-heat	−2.9 (1.6)	+2.1 (1.2)	−1.5 (10.0)	−2.0 (8.7)	−0.6 (2.2)	−13.9 (1.6)	+11.7 (1.8)
Latent-heat	−1.4 (3.1)	+0.5 (1.7)	−5.8 (6.4)	−4.7 (4.0)	+8.3 (5.4)	−11.5 (1.7)	+9.7 (1.3)

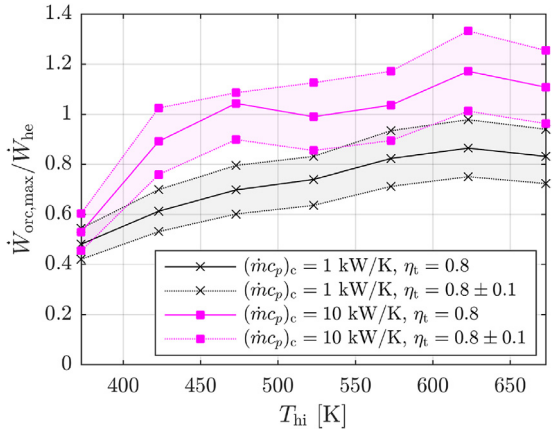

Fig. 7. Sensitivity of the sensible-heat validation study to the turbine efficiency used for the ORC optimisation.

discrete nature of fluid selection. Referring to Fig. 6, the same conclusions are found for the latent-heat comparison, although the deviation between the two models is much lower.

To investigate the sensitivity of the ORC optimisation study to the assumed component efficiencies a sensitivity study concerning the pump and turbine efficiencies and the recuperator effectiveness was carried out. The results are summarised in Table 3. It is observed that the results are not significantly affected by the pump or recuperator effectiveness, with percentage deviations between −5.8% and +2.51% (neglecting the latent-heat $\varepsilon_r = 1.0$ case which represents an impractical cycle). However, the results are more sensitive to the turbine efficiency, with a decrease or increase in turbine efficiency of 10% corresponding to percentage deviations in the ranges of −13.9% to −11.5% and +9.6% and +11.7% respectively. However, the standard deviations are small, indicating that this shift is relatively uniform across the different heat-source and heat sink conditions, as observed from the results shown in Fig. 7. Moreover, from this figure it is observed that for a sufficiently large heat sink (*i.e.*, $(\dot{m}c_p)_c = 10$ kW/K) the ORC power remains within ± 20% of the heat-engine model for the majority of the heat-source and heat-sink conditions. The same behaviour is observed in the equivalent plot for the latent-heat systems, but has not been reported for brevity.

Overall, the validation study suggests that the sensible- and latent-heat heat-engine models provide a good indication of the power that could be obtained using an ORC system, provided that the heat-source temperature is sufficiently high and the heat sink is sufficiently large. It is worth noting that in most applications $(\dot{m}c_p)_c >> (\dot{m}c_p)_h$, whilst heat-source temperatures of 373 K are perhaps on the lower limit of economic viability for power generation. Thus, the model is deemed sufficient as a first-stage assessment.

A final validation study concerns cascaded HE-TES systems, in which the ORC optimisation study has been repeated for two-stage and three-stage TES systems, using the same inputs and assumptions defined in Tables 1 and 2. The temperature of the first TES stage is set to $\theta_1 = 1$, whilst values for the second and third stages are varied within the range of 0.5 to 0.9. For the two-stage systems, the total heat-transfer rate is divided across the two-stages with different ratios, corresponding to 2:1, 1:1 and 1:2. For the three-stage systems, the total heat-transfer rate is divided across the three-stages with ratios of 1:1:1, 1:1:2, 1:2:1 and 2:1:1. The results from this study are reported in Fig. 8. These results echo those observed for the single-stage systems, with low heat-source temperatures and low heat-sink heat-capacity rates corresponding to larger deviations. However, for sufficiently large heat sinks ($(\dot{m}c_p)_c \geq 5$ kW/K), and heat-source temperatures exceeding 373 K, the majority of the results agree within ± 10%. However, it is observed that the deviation appears to increase as the number stages is increased.

3. Case studies

Within this study, two case studies are considered. In the first, two mock heat-source profiles are constructed that are representative of potential applications where HE-TES systems may be installed. This allows the effect of the heat-source temperature and heat-capacity ratio on the optimal design and performance of the system to be studied in detail, which, in turn, provides insight into the general behaviour of these systems. In the second case study, the models are applied to real heat sources taken from the literature, and are therefore of direct industrial relevance.

3.1. Case study 1 definition

For this first cast study, the heat-source profiles shown in Fig. 9 have been defined. The first profile (Fig. 9a) represents a batch, or cyclic, process where the flow of waste heat is only available at certain points in time, but when it is, it is available at a constant temperature and mass-flow rate. This waste-heat stream is represented as a square signal, and is shown in a non-dimensional form so it can be applied to any arbitrarily defined heat-source mass-flow rate (*i.e.*, $\dot{m}_h(t)/\dot{m}_{h,av}$, where $\dot{m}_{h,av}$ is the average, or steady-state, mass-flow rate). The second profile (Fig. 9b) represents a waste-heat stream that is varying periodically. Again, the mass-flow rate function is given in a non-dimensional form, whilst the temperature fluctuation is defined as the difference between the heat-source temperature at a given time and the average, or steady-state, temperature (*i.e.*, $\Delta T_h(t) = T_h(t) - T_{h,av}$). The heat-source profiles have been defined over a period of one hour, since, from a thermodynamic point of view, if the same heat source profile was imposed over the timescale of a few minutes or a few hours the normalised energy production (*i.e.*, E/E_{max}) would be the same. The timescale would affect the heat-transfer process within the latent-heat thermal-energy storage system, but this aspect is not considered within this study.

The performance of a HE-TES system will be evaluated for these two heat-source profiles for a range of heat-source and heat-sink conditions, as summarised in Table 4. For each condition, the system performance can be evaluated for different TES temperatures,

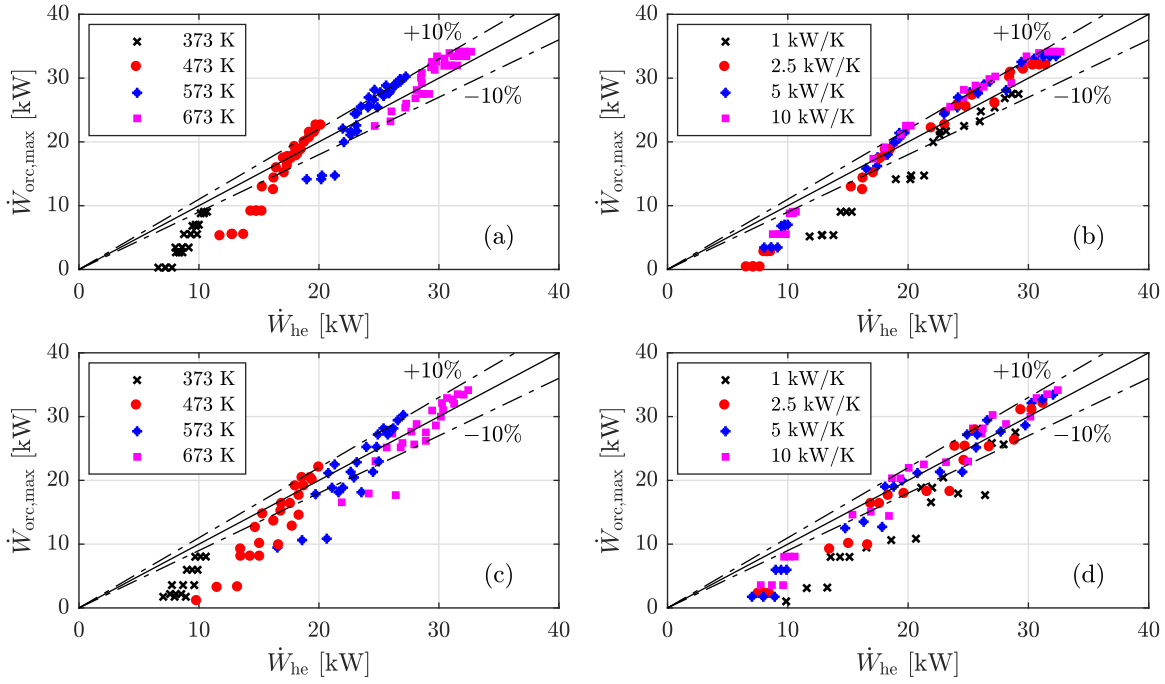

Fig. 8. Validation of the model for heat engines operating with cascaded TES: (a) and (b) refer to a two-stage cascaded systems; (c) and (d) refer to a three-stage cascaded system.

Table 4
Heat-source and heat-sink conditions for case study 1.

$T_{\mathrm{h,av}}$ [K]	T_{ci} [K]	$\dot{m}_{\mathrm{h,av}}$ [kg/s]	γ	$c_{p,\mathrm{h}}$, $c_{p,\mathrm{c}}$ [kJ/(kg K)]
373–673	288	1	1, 2, 5, ∞	1

T_{tes}, defined with the following non-dimensional form:

$$\theta_{\mathrm{tes}} = \frac{T_{\mathrm{h,av}} - T_{\mathrm{tes}}}{T_{\mathrm{h,av}} - T_{\mathrm{ci}}}. \tag{14}$$

3.2. Results for a 473 K heat source

The effect of θ_{tes} and γ on the total energy produced by a HE-TES system operating with a 473 K heat source is considered first. In Fig. 10a and Fig. 10b the results for the two different heat-source profiles are normalised by $E_{\mathrm{max},\infty}$, which is the maximum energy that could be produced using a heat engine that adapts instantaneously to heat-source fluctuations and for which $\gamma \to \infty$; this represents an estimate of the maximum energy that could be produced from the available waste-heat stream. In Fig. 10c and Fig. 10d, the results are normalised by E_{max}, which is the maximum energy that could be produced using a heat engine that adapts instantaneously to heat-source fluctuations but with the same heat-sink heat-capacity rate.

Referring to Fig. 10, there exists an optimal temperature, θ_{tes}, for a latent-heat TES system that results in the highest energy production. This optimum ranges between 0.35 and 0.6 depending on the type of heat source, and on γ, and exists because of the trade-off depicted in Fig. 1. It is also noted that the total energy production for a HE-TES system is always less than an optimal heat engine that converts the waste heat into power directly. This is not surprising, and is the result of a number of effects. Firstly, for the heat to be transferred from the waste-heat source to the heat engine, the waste-heat source first transfers heat to the isothermal heat-storage medium, and then the isothermal heat-storage medium transfers heat to the heat engine;

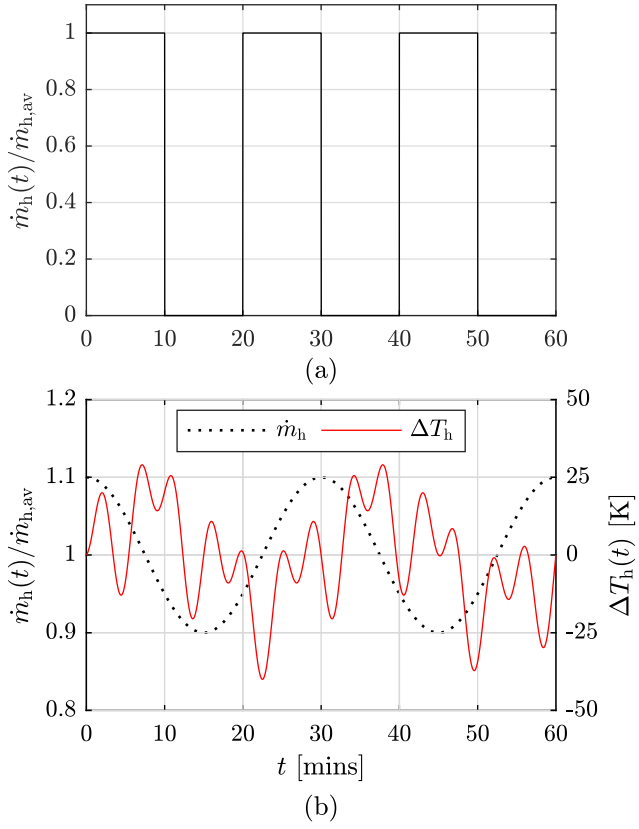

Fig. 9. Heat-source profiles defined for case study 1: (a) batch, or cyclic, process; (b) fluctuating heat source. Profiles are defined in terms of a non-dimensional mass-flow rate, $\dot{m}_{\mathrm{h}}(t)/\dot{m}_{\mathrm{h,av}}$, and a temperature fluctuation, $\Delta T_{\mathrm{h}}(t) = T_{\mathrm{h}}(t) - T_{\mathrm{h,av}}$, where $\dot{m}_{\mathrm{h,av}}$ and $T_{\mathrm{h,av}}$ are the average, or steady state, conditions.

both of these heat-transfer processes are associated with an exergy loss, and hence a reduction in power output. This is further exacerbated by the isothermal nature of the storage medium. Secondly, the inclusion of a storage medium lowers the average

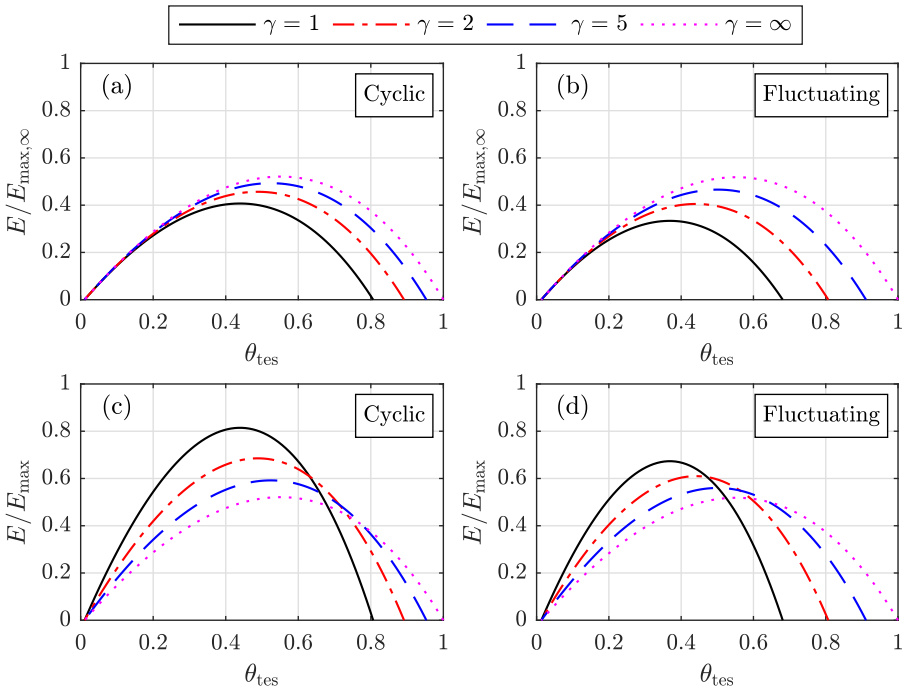

Fig. 10. Effect of the thermal-energy storage temperature θ_{tes} and heat-capacity ratio γ on the energy produced from a HE-TES system for a heat-source temperature of 473 K. Plots on the left-hand side correspond to the cyclic heat source (Fig. 9a) and plots on the right-hand side correspond to the fluctuating heat source (Fig. 9b).

temperature of heat addition into the heat engine, which lowers the heat engine thermal efficiency. This reduces the power output, but also subsequently increases the amount of heat rejected to the sink, and in turn increases the average temperature of heat rejection. These effects result in the total energy produced by the HE-TES system ranging between 30% and 60% of the total could theoretically be produced for an infinitely large heat sink, $E_{max,\infty}$.

It is observed from Fig. 10a and Fig. 10b that the energy production from the HE-TS system reduces as γ reduces. Whilst this is true, these figures give a slightly skewed picture as all systems are compared to the heat engine operating with $\gamma \to \infty$. When comparing the HE-TES systems to heat engines operating with the same size heat sink (Fig. 10c and Fig. 10d), it is observed that the performance of the HE-TES system, relative to a heat engine operating with the same heat source and heat sink, actually improves as γ reduces. For example, for the cyclic heat source with $\gamma = 5$ it is predicted that an optimal HE-TES system would produce 60% of the energy that could be produced using a heat engine directly. However, if γ reduces to unity it is predicted that the optimal HE-TES system would produce 80% of the energy that could be produced using a heat engine. In other words, these results suggest that HE-TES systems appear to be a more suitable option for applications where γ is low.

Finally, comparing the two different heat-source profiles, the optimal HE-TES systems for the cyclic heat source are associated with higher values of θ_{tes}, and produce more energy than the systems for the fluctuating heat source. Moreover, the HE-TES system with the best relative performance is found for the cyclic heat source with $\gamma = 1$. These results suggest that applications that involve a cyclic, or batch process, and have a limited heat sink available represent a promising area for HE-TES systems. Excluding this case, the remaining results are quite similar, which suggests that the optimal values of θ_{tes} and $E/E_{max,\infty}$ are more significantly affected by the heat-sink conditions (*i.e.,* γ), than the variability of the heat-source.

3.3. Results for other heat-source temperatures

Extending the analysis to a wider range of heat-source temperatures, and in each case finding the optimal value for θ_{tes}, the results shown in Fig. 11 are obtained. In Fig. 11a and Fig. 11b the optimal value for θ_{tes} for different heat-source temperatures and heat-capacity ratios are shown, whilst in Fig. 11c and Fig. 11d the results for the normalised total energy production are shown.

The first observation is that the optimal value of θ_{tes}, and the normalised energy production, both increase slightly as $T_{h,av}$ increases, but on the whole are not significantly affected by $T_{h,av}$. However, both are affected by γ. This reaffirms that the precise nature of the heat-source profile, and the average temperature of the heat-source, do not have a significant affect on the optimal operation of a latent-heat HE-TES system. Instead, the optimal system is largely dependent on the available heat sink.

The results from Figs. 10 and 11 show that, compared to a heat engine without TES that adapts instantaneously to changes in the heat source, employing latent-heat TES will lead to a reduction in the total energy that could be produced from the system. However, for the heat engine without TES to fully exploit all the available waste heat, it must be sized for the maximum power point. In comparison, for the HE-TES system, the heat engine operates in a steady state, and hence its rated power is lower. Moreover, operating at a steady state has advantages with regards to the required control strategy. Hence, it is interesting to compare the power ratings for the heat engines operating with and without TES, as shown in Fig. 12.

For the cyclic heat-source profile the rated power of the HE-TES system ranges between 25% and 40% of the rated power of the optimal heat engine operating without TES, depending $T_{h,av}$ and γ. For the fluctuating heat-source profile, the results show more variation, and range approximately between 30% and 60% of the optimal heat engine rated power. Therefore, it appears that implementing TES allows a significant reduction in the power rating of the heat engine; however, it should be remembered that this is

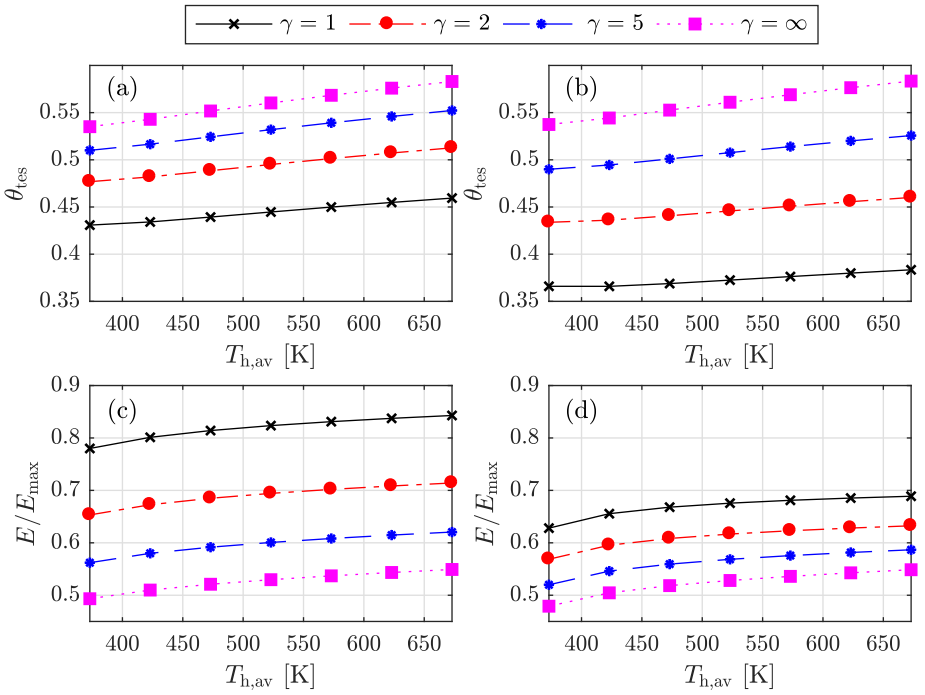

Fig. 11. Optimal latent-heat thermal-energy storage systems for different heat-source temperatures, $T_{h,av}$ and heat-capacity ratios γ, shown in terms of the optimal TES temperature and normalised energy production. Plots on the left-hand side correspond to the cyclic heat source (Fig. 9a) and plots on the right-hand side correspond to the fluctuating heat source (Fig. 9b).

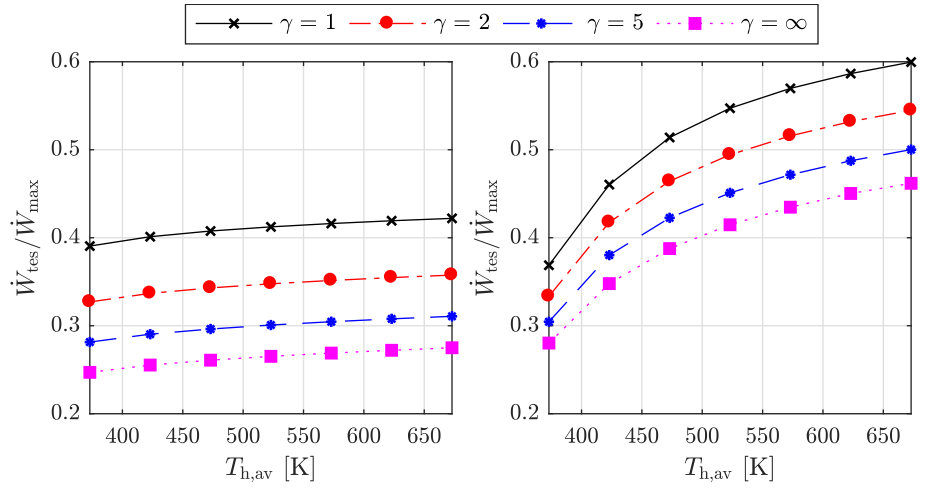

Fig. 12. Comparison between the power rating of the required HE-TES system, $\dot{W}_{tes}$, and the power rating of an optimal heat engine operating without TES that adapts instantaneously to the heat-source conditions, $\dot{W}_{max}$. Plots on the left-hand side correspond to the cyclic heat source (Fig. 9a) and plots on the right-hand side correspond to the fluctuating heat source (Fig. 9b).

associated with a reduction in the overall energy that can be produced (Fig. 11c and Fig. 11d).

For the cyclic heat-source profile, it is observed that power ratings are not affected by $T_{h,av}$, but are affected by γ, which is in line with the findings previously discussed. For the fluctuating heat-source profile, there is slightly more variation in the results. In particular, as $T_{h,av}$ reduces to below 500 K, the relative power rating of the heat engine within the HE-TES systems reduces relatively rapidly. By way of example, consider the results for T_{av} equal to 423 K and 673 K with $\gamma = 1$. For the 673 K case the HE-TES system produces around 70% of the maximum energy that could be produced (Fig. 11d), whilst the relative power rating of the system is 60%. In comparison, for the 423 K case, the HE-TES produces around 65% of the maximum energy that could be produced, whilst the relative power rating is reduced to 45%. Similar results are observed for larger heat-capacity ratios, although the results are less significant. This suggests that low-temperature, fluctuating heat sources offer the largest potential in terms of downsizing the heat engine.

3.4. Wider economic perspectives

Considering Figs. 11 and 12 it appears that, in applications with a high average heat-source temperature and low heat-sink availability, a HE-TES system could generate a large proportion of the maximum energy that is available. However, these systems need to be sized with a relatively large power rating to achieve this energy production. The two factors of total energy production and

power rating are linked, since a heat engine with a higher power rating that operates under a constant, full-load condition, will generate more energy over its lifetime. However, the question arises whether downsizing the system and installing TES represents a more economic option than installing a heat engine that is rated for the maximum power point and is adequately controlled such that it effectively tracks the changes in the heat-source conditions.

The total energy production is linked to the revenue that can be generated over the systems lifespan, whilst the power rating is linked to the capital costs associated with the installation, operation and maintenance of the system. These two factors can be linked by considering the payback period, defined as:

$$\mathrm{PB} = \frac{C_0}{P} = \left(\frac{\mathrm{SIC}}{nC_\mathrm{e}}\right)\frac{\dot{W}}{E}, \tag{15}$$

where PB is the payback period, C_0 is the total investment cost, P is the revenue per year, SIC is the system specific investment cost (in £/kW), n is the number of operational hours and C_e is the net profit per kWh of electricity generated. If SIC, n and C_e are assumed constant, it follows that $\mathrm{PB} \propto \dot{W}/E$. Hence, the ratio $\dot{W}/E$ is useful as a preliminary assessment of economic performance.

For the HE-TES systems, $\dot{W}/E = 1$, since the heat-source profiles are defined for the duration of one hour, whilst the heat-engine is assumed to operate under a constant, full-load condition for the entire duration. For the optimal heat engine for the cyclic heat source, $\dot{W}/E = 2$, since the heat engine is sized for the maximum power point (*i.e.*, $\dot{m}_\mathrm{h} = 1$ kg/s), but only generates power half of the time. For the fluctuating heat source, the results for the optimal heat engines sized for the maximum power point and operating without TES are shown in Fig. 13. From this, it is observed that $\dot{W}/E$ ranges between approximately 1.2 and 1.7 kW/kWh and is strongly dependent on the average heat-source temperature. However, the results are not significantly affected by γ, which means the effects shown in Figs. 11d and 12 effectively cancel out.

The results in Fig. 13 suggest that for the fluctuating heat source, if SIC, n, C_e are assumed constant, the payback period for the optimal heat engines will be between 1.2 and 1.7 times larger than the payback for the HE-TES systems. For the cyclic heat source, for which $\dot{W}/E = 2$, the optimal heat engines will have twice the payback period of the HE-TES systems. However, in reality the HE-TES system will have a larger SIC than the optimal heat engines, due to the cost of the TES system and the additional infrastructure required to couple the TES system to the heat engine and heat source. Therefore, Eq. (15) can be rearranged to calculate how much larger the SIC for the HE-TES can be in order to obtain the same payback:

$$\mathrm{SIC}_\mathrm{tes} = \mathrm{SIC}_\mathrm{max}\left(\frac{(\dot{W}_\mathrm{max}/E_\mathrm{max})}{(\dot{W}_\mathrm{tes}/E_\mathrm{tes})}\right). \tag{16}$$

Referring back to Fig. 13, it follows that the SIC for the 373 K HE-TES systems should be kept below 1.7 times the SIC for the optimal heat engine, whilst for the 673 K it should be kept below 1.2 times the SIC for the optimal heat engine. If the SIC of the heat engine in either case is assumed equal, it follows that for the 373 K and 673 K cases, the total cost of the TES system should not exceed 70% and 20% of the total cost of the heat engine unit, respectively, for the HE-TES system to obtain the same payback period. For the cyclic heat source, the total cost of the TES system should not exceed the cost of the heat engine.

3.5. Results for cascaded systems

A preliminary investigation into cascaded systems has been completed for the fluctuating heat source with $T_\mathrm{h,av} = 473$ K and $\gamma = 5$. In Fig. 14a, the effect of the TES temperatures on the total energy production from a two-stage TES system is shown, from which it is observed that at $\theta_1 = 0.3$ and $\theta_2 = 0.6$ maximum energy is produced, and this is approximately 70% of the maximum that could be obtained using an optimal heat engine without TES. The effect of the number of stages on the maximum power that can be generated is shown in Fig. 14b. These results show that increasing the number of stages leads to a larger total energy production, although after a number of stages, the relative improvement is diminished.

The results for cascaded systems have been included to demonstrate the potential of the method developed within this paper to simulate cascaded TES systems. As such, it is noted that introducing cascaded systems is likely to improve thermodynamic performance, but it is acknowledged that this will introduce more

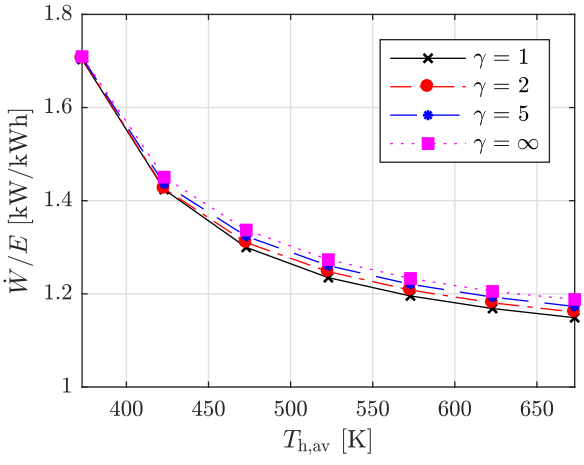

Fig. 13. Effect of $T_\mathrm{h,av}$ and γ on the ratio of system power rating to energy produced, $\dot{W}/E$, for an optimal heat engine operating without TES that adapts instantaneously to the heat-source conditions.

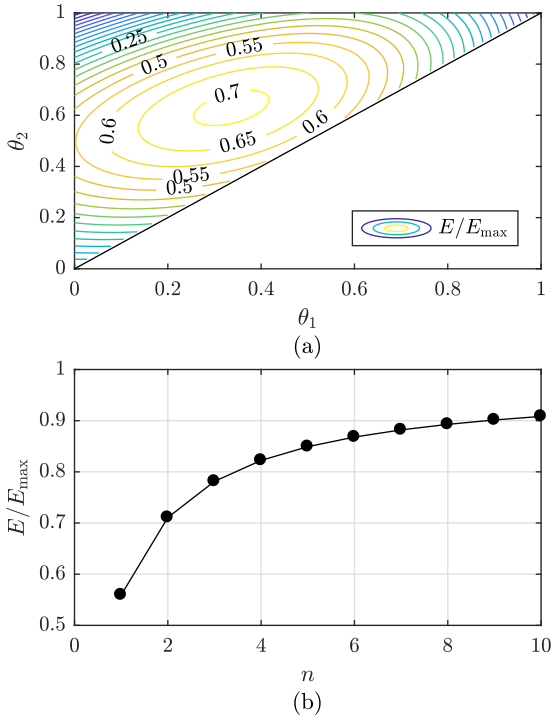

Fig. 14. Results for case-study 1(b), with $T_\mathrm{h,av} = 473$ K and $\gamma = 5$: (a) effect of TES temperatures on energy production for a two-stage TES system; (b) effect of the number of TES stages on energy production where each result refers to the optimal set of TES temperatures identified through optimisation.

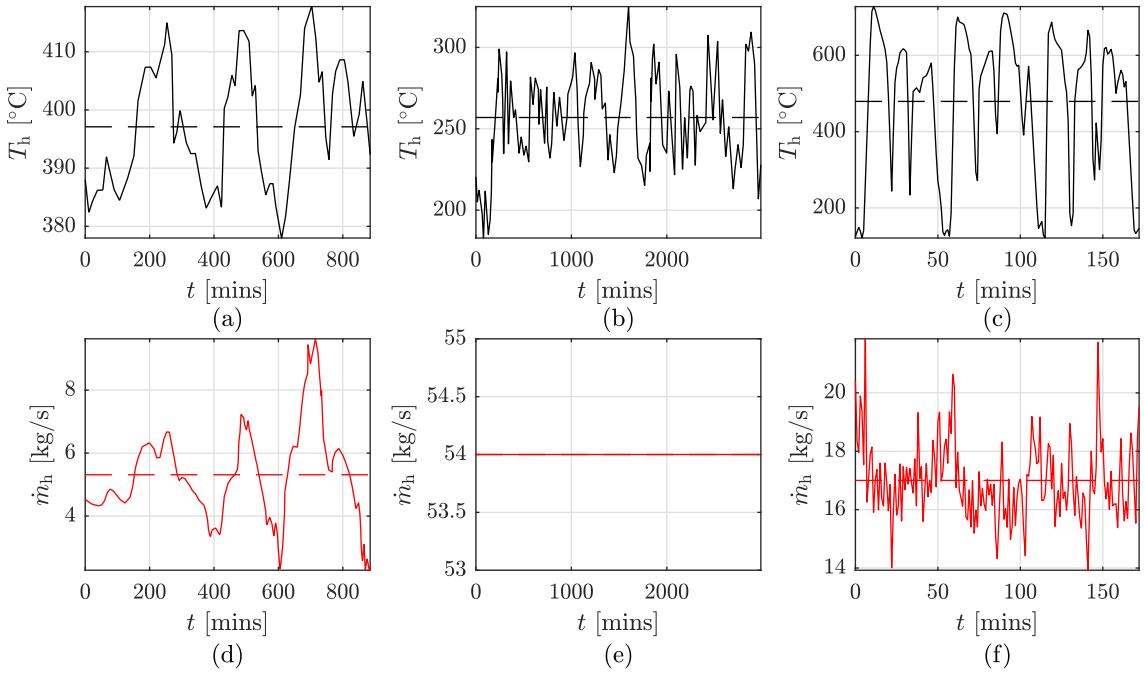

Fig. 15. Industrial waste-heat streams, taken from Ref. [23], defined by the heat-source temperature (a–c) and mass-flow rate (d–f): (a) and (d) refer to a steel billet reheating furnace [22]; (b) and (e) refer to a clinker cooler [42]; (c) and (f) refer to an electric-arc furnace [43].

complexity into the design of the system and increase the power rating of the heat engine; both of which have implications in terms of the system economics. A more detailed investigation into cascaded systems is left for future investigations.

3.6. Case study 2: Practical case studies

For the second case study, the developed model will be applied to real waste-heat streams studied within the literature. The waste-heat streams in question are shown in Fig. 15. This data been extracted from Ref. [23], but originally relate to studies on three different industrial processes [22,42,43]. From left to right, the heat sources will be referred to as heat-source 1, 2 and 3 respectively. For each heat source, the analysis completed for case study 1 has been repeated to evaluate the performance of a HE-TES system. More specifically, this involved a parametric investigation into the effects of θ_{tes} and γ on the performance of the system. It is again assumed that the heat-sink is available at a temperature of $T_{ci} = 288$ K.

For brevity, the results from this study are not shown graphically here as the results are almost identical to those reported in Fig. 10, and are very similar for all three heat sources. When comparing the optimal value for θ_{tes} for each case it is found that the optimal values for the $\gamma = 1$ cases range between 0.37 and 0.39, whilst the optimal values for the $\gamma = \infty$ range between 0.57 and 0.60. The corresponding normalised energy production values (E/E_{max}) range between 0.68 and 0.72 for the $\gamma = 1$ cases, and 0.52 and 0.55 for the $\gamma = \infty$ cases. Ultimately, this, alongside the similarity between these results and those reported in Fig. 10, suggests that the results within this study are broadly applicable to any HE-TES system, and can inform the selection of a suitable value for θ_{tes} for any waste-heat stream. This can be confirmed by combining the results from case study 1 and case study 2; the optimal values of θ_{tes} for every combination of heat source and heat-capacity ratio are summarised in Fig. 16, alongside the normalised energy production (E/E_{max}). In this figure, case study 1(a) and 1(b) refer to the cyclic and fluctuating heat-source profiles respectively. Ultimately, the very small spread in the optimal value θ_{tes}, particularly

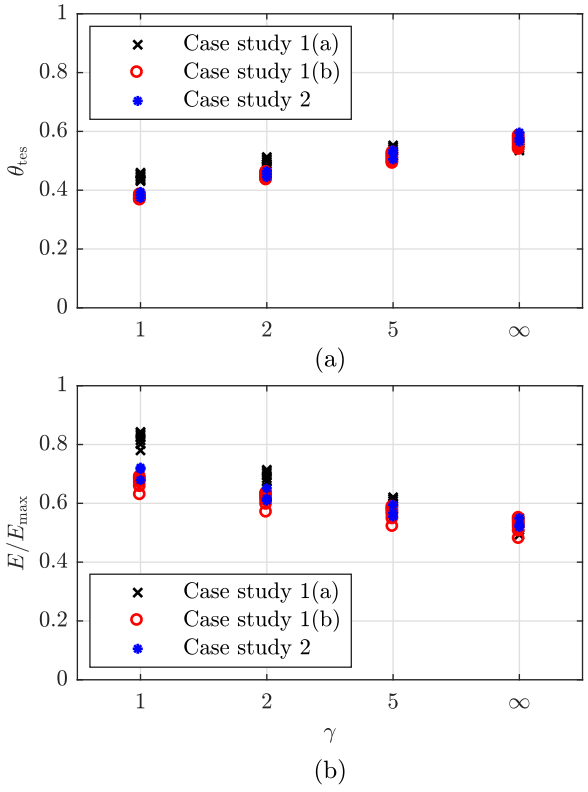

Fig. 16. Optimal HE-TES systems identified within this study: (a) optimal value of θ_{tes}; (b) normalised energy production.

for case studies 1(b) and 2, confirms the validity of extrapolating these results to other heat-sources. This result is particularly encouraging given the relatively large variability in the average values and range for both $T_{h,av}$ and $\dot{m}_{h,av}$ that have been considered within this study.

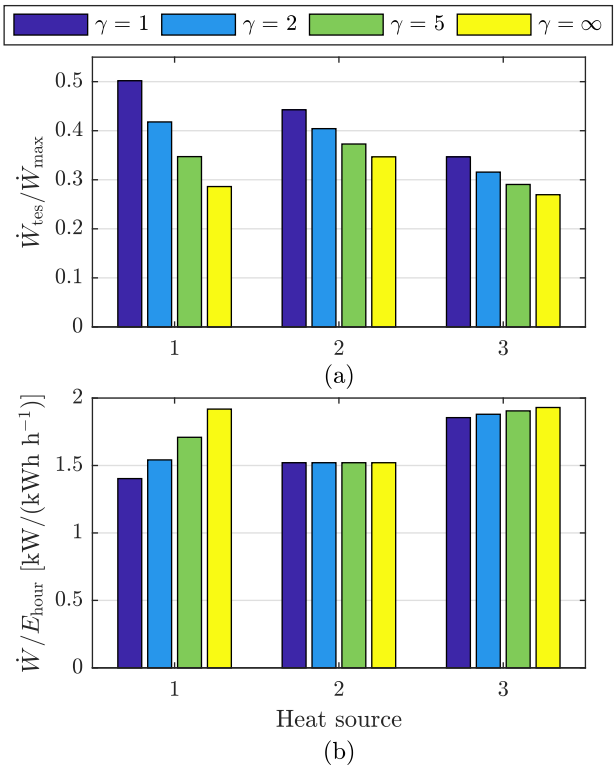

Fig. 17. Comparison between optimal HE-TES systems and heat engines operating without TES: (a) normalised power rating of the HE-TES system; (b) preliminary payback period comparison.

To conclude the second case study, the power ratings for the optimal HE-TES systems for each heat source have been compared to the power rating required for an optimal heat engine without TES (Fig. 17a). Moreover, the ratio, $\dot{W}/E$, has been shown for the three different heat sources. It should be noted that unlike the heat source considered in case study 1, the heat source in case study 2 are defined over longer periods of time than an hour. Therefore, to be consistent with the results presented in Fig. 13, the energy production used in Fig. 17b is the average energy production per hour. In summary, the results in Fig. 17a echo the findings from case study 1. This it to say, as γ increases, the power rating of the HE-TES system is reduced, relative to the size of the optimal heat engine operating without TES. Moreover, for all cases apart from the $\gamma = 1$ case for heat-source 1, the ratio of the power rating of the optimal heat engine, to the total energy produced per hour is greater than 1.5 kW/(kWh h^{-1}), suggesting that if the cost of the TES system does not exceed 50% of the total cost of the heat-engine unit, the HE-TES system should achieve the same, if not lower, payback period than an optimal heat engine that is rated for the maximum power point and is capable of effectively tracking the heat-source variability.

4. Conclusions

Within this paper, a new method to provide fast and accurate estimates of the performance of heat engines coupled to latent-heat thermal-energy storage (HE-TES) for waste-heat recovery applications has been presented. The method can identify the optimal temperature of the latent-heat TES systems based only on the heat-source and heat-sink conditions, and can evaluate single-stage and cascaded TES systems. Validation of the model against optimal organic Rankine cycle systems shows that for sufficiently large heat sinks (*i.e.*, $(\dot{m}c_p)_c/(\dot{m}c_p)_h \geq 5$) and heat-source temperatures exceeding 373 K, the results agree to within $\pm$ 10%. After applying the method to a range of waste-heat streams, the following conclusions are made:

- For a given application there exists an optimal latent-heat TES temperature. The optimal non-dimensional temperature, $\theta_{\mathrm{tes}} = (T_{\mathrm{h,av}} - T_{\mathrm{tes}})/(T_{\mathrm{h,av}} - T_{\mathrm{ci}})$, is not significantly affected by the heat-source temperature, but is affected by the size of the heat sink, ranging between 0.36 and 0.46 for $(\dot{m}c_p)_c = (\dot{m}c_p)_h$, and 0.53 and 0.60 for $(\dot{m}c_p)_c \to \infty$.
- The normalised energy production, E/E_{max}, reduces as the size of the heat sink increases, ranging between 0.62 and 0.85 for $(\dot{m}c_p)_c = (\dot{m}c_p)_h$, and 0.47 and 0.55 for $(\dot{m}c_p)_c \to \infty$. This suggests applications with relatively small heat sinks could be optimal candidates for HE-TES systems.
- The power ratings for HE-TES systems range between 25% and 60% of the power ratings for optimal heat engines operating without TES that accurately track waste-heat fluctuations, and are associated with a reduction in the total energy production that ranges between 45% and 85% respectively.
- A preliminary economic evaluation has been completed to predict the maximum allowable cost for the TES system to obtain the same payback period as an optimal heat engine operating without TES. For case study 2, it is found that if the cost of the TES system does not exceed 50% of the cost of the heat-engine unit, the HE-TES systems could achieve a similar, if not lower, payback period.

Overall, cyclic processes with only small heat sinks available appear to be a favourable application for HE-TES systems. However, the small deviation between the results obtained for each heat source suggests that the results are broadly applicable to most heat-source profiles. This gives good confidence in the validity of extrapolating the results to other heat-sources that have not been considered within the current study.

Declaration of Competing Interest

We wish to confirm that there are no known conflicts of interest associated with this publication and there has been no significant financial support for this work that could have influenced its outcome.

We confirm that the manuscript has been read and approved by all named authors and that there are no other persons who satisfied the criteria for authorship but are not listed. We further confirm that the order of authors listed in the manuscript has been approved by all of us.

We confirm that we have given due consideration to the protection of intellectual property associated with this work and that there are no impediments to publication, including the timing of publication, with respect to intellectual property. In so doing we confirm that we have followed the regulations of our institutions concerning intellectual property.

We understand that the Corresponding Author is the sole contact for the Editorial process (including Editorial Manager and direct communications with the office). He is responsible for communicating with the other authors about progress, submissions of revisions and final approval of proofs. We confirm that we have provided a current, correct email address which is accessible by the Corresponding Author and which has been configured to accept email from martin.white@city.ac.uk.

Acknowledgements

This work was supported by the UK Engineering and Physical Sciences Research Council (EPSRC) [grant number: EP/P009131/1].

References

[1] European Union, The strategic energy technology (SET) plan, Technical Report, European Union, 2017, doi:10.2777/48982.

[2] EASE/EERA, European energy storage technology development roadmap - 2017 update, Technical Report, EASE/EERA, Brussels, 2017.

[3] B. Sanner, K. Ria, A. Land, K. Mutka, P. Papillon, G. Stryi-Hipp, W. Weiss, Common vision for the renewable heating & cooling sector in Europe, Technical Report, European Union, 2011, doi:10.2788/20474.

[4] Delta Energy & Environment Ltd., Evidence gathering: thermal energy storage (TES) technologies, Technical Report, Department for Business, Energy & Industrial Strategy, 2016.

[5] I. Sarbu, C. Sebarchievici, A comprehensive review of thermal energy storage, Sustainability 10 (1) (2018) 191, doi:10.3390/su10010191.

[6] S. Seddegh, X. Wang, A.D. Henderson, Z. Xing, Solar domestic hot water systems using latent heat energy storage medium: a review, Renew. Sustain. Energy Rev. 49 (2015) 517–533, doi:10.1016/j.rser.2015.04.147.

[7] U. Pelay, L. Luo, Y. Fan, D. Stitou, M. Rood, Thermal energy storage systems for concentrated solar power plants, Renew. Sustain. Energy Rev. 79 (January) (2017) 82–100, doi:10.1016/j.rser.2017.03.139.

[8] D. Iaria, J. Alzaili, A.I. Sayma, Solar dish micro gas turbine technology for distributed power generation, in: S. De, S. Bandyopadhyay, M. Assadi, D.A. Mukherjee (Eds.), Sustainable Energy Technology and Policies, Springer, Singapore, 2018, pp. 119–131, doi:10.1007/978-981-10-7188-1_5.

[9] S. Quoilin, M. van den Broek, S. Declaye, P. Dewallef, V. Lemort, Techno-economic survey of organic rankine cycle (ORC) systems, Renew. Sustain. Energy Rev. 22 (1) (2013) 168–186.

[10] F. Crespi, G. Gavagnin, D. Sánchez, G.S. Martínez, Supercritical carbon dioxide cycles for power generation: a review, Appl. Energy 195 (2017) 152–183, doi:10.1016/j.apenergy.2017.02.048.

[11] I. Johnson, W.T. Choate, Waste Heat Recovery: Technology and Opportunities in U.S. Industry, Technical Report, BCS, Incorporated, 2008, doi:10.1017/CBO9781107415324.004.

[12] R.C. McKenna, Industrial Energy Efficiency: Interdisciplinary Perspectives on the Thermodynamic, Technical and Economic Constraints, University of Bath, 2009 Phd.

[13] Element Energy, The Potential for Recovering and using Surplus Heat from Industry, Technical Report, Department for Energy and Climage Change, London, UK, 2014.

[14] G.Y. Ma, J.J. Cai, W.W. Zeng, H. Dong, Analytical research on waste heat recovery and utilization of china's iron & steel industry, Energy Procedia 14 (2012) 1022–1028, doi:10.1016/j.egypro.2011.12.1049.

[15] F. Campana, M. Bianchi, L. Branchini, A. De Pascale, A. Peretto, M. Baresi, A. Fermi, N. Rossetti, R. Vescovo, ORC Waste heat recovery in european energy intensive industries: energy and GHG savings, Energy Convers. Manage. 76 (1) (2013) 244–252.

[16] J. Freeman, I. Guarracino, S. Kalogirou, C. Markides, A small-scale solar organic rankine cycle combined heat and power system with integrated thermal-energy storage, Appl. Therm. Eng. 127 (2017) 1543–1554, doi:10.1016/j.applthermaleng.2017.07.163.

[17] J.M. Rodríguez, D. Sánchez, G.S. Martínez, E.G. Bennouna, B. Ikken, Techno-economic assessment of thermal energy storage solutions for a 1 MWe CSP-ORC power plant, Sol. Energy 140 (2016) 206–218, doi:10.1016/j.solener.2016.11.007.

[18] L. Miró, J. Gasia, L.F. Cabeza, Thermal energy storage (TES) for industrial waste heat (IWH) recovery: a review, Appl. Energy 179 (2016) 284–301, doi:10.1016/j.apenergy.2016.06.147.

[19] E.A. Bufi, S. Camporeale, F. Fornarelli, B. Fortunato, A.M. Pantaleo, A. Sorrentino, M. Torresi, Parametric multi-objective optimization of an organic rankine cycle with thermal energy storage for distributed generation, Energy Procedia 126 (2017) 429–436, doi:10.1016/j.egypro.2017.08.239.

[20] S. Lecompte, O.A. Oyewunmi, C.N. Markides, M. Lazova, A. Kaya, M. Van Den Broek, M. De Paepe, Case study of an organic rankine cycle (ORC) for waste heat recovery from an electric arc furnace (EAF), Energies 10 (5) (2017) 1–16, doi:10.3390/en10050649.

[21] A.M. Pantaleo, J. Fordham, O.A. Oyewunmi, P. De Palma, C.N. Markides, Integrating cogeneration and intermittent waste-heat recovery in food processing: microturbines *vs.* ORC systems in the coffee roasting industry, Appl. Energy 225 (April) (2018) 782–796, doi:10.1016/j.apenergy.2018.04.097.

[22] F. Dal Magro, M. Jimenez-Arreola, A. Romagnoli, Improving energy recovery efficiency by retrofitting a PCM-based technology to an ORC system operating under thermal power fluctuations, Appl. Energy 208 (10) (2017) 972–985, doi:10.1016/j.apenergy.2017.09.054.

[23] M. Jiménez-Arreola, R. Pili, F. Dal Magro, C. Wieland, S. Rajoo, A. Romagnoli, Thermal power fluctuations in waste heat to power systems: an overview on the challenges and current solutions, Appl. Therm. Eng. 134 (February) (2018) 576–584, doi:10.1016/j.applthermaleng.2018.02.033.

[24] H. Zhai, Q. An, L. Shi, V. Lemort, S. Quoilin, Categorization and analysis of heat sources for organic rankine cycle systems, Renew. Sustain. Energy Rev. 64 (2016) 790–805, doi:10.1016/j.rser.2016.06.076.

[25] H. Michels, R. Pitz-Paal, Cascaded latent heat storage for parabolic trough solar power plants, Sol. Energy 81 (6) (2007) 829–837, doi:10.1016/j.solener.2006.09.008.

[26] H.J. Xu, C.Y. Zhao, Thermal efficiency analysis of the cascaded latent heat/cold storage with multi-stage heat engine model, Renew. Energy 86 (2016) 228–237, doi:10.1016/j.renene.2015.08.007.

[27] I.I. Novikov, The efficiency of atomic power stations (A review), J. Nuclear Energy II 7 (1–2) (1958) 125–128, doi:10.1016/0891-3919(58)90244-4.

[28] F.L. Curzon, B. Ahlborn, Efficiency of a carnot engine at maximum power output, Am. J. Phys. 43 (22) (1975) 22–24 https://doi.org/10.1119/1.10023.

[29] M.H. Rubin, Optimal configuration of a class of irreversible heat engines. i, Phys. Rev. A 19 (3) (1979) 1272–1276.

[30] M.H. Rubin, Optimal configuration of a class of irreversible heat engines. II, Phyis. Rev. A 19 (3) (1979) 1277–1289.

[31] M.J. Ondrechen, M.H. Rubin, Y.B. Band, The generalized carnot cycle : a working fluid operating in finite time between finite heat sources and sinks, J. Chem. Phys. 78 (1983) 4721–4727, doi:10.1063/1.445318.

[32] C. Wu, Power optimization of a finite-time Carnot heat engine, Energy 13 (9) (1988) 681–687.

[33] M. Ibrahim, S.A. Klein, J.W. Mitchell, Optimum heat power cycles for specified boundary conditions, J. Eng. Gas Turbine. Power 113 (1991) 515–521.

[34] J. Chen, The maximum power output and maximum efficiency of an irreversible carnot heat engine, J. Phys. D 27 (1994) 1144–1149.

[35] R. Long, W. Liu, Ecological optimization for general heat engines, Phys. A 434 (2015) 232–239, doi:10.1016/j.physa.2015.04.016.

[36] F.A. Brown, An ecological optimization criterion for finitetime heat engines, J. Appl. Phys. 69 (11) (1991) 7465–7469, doi:10.1063/1.347562.

[37] S.C. Kaushik, S. Kumar, Finite time thermodynamic analysis of endoreversible stirling heat engine with regenerative losses, Energy 25 (2000) 989–1003.

[38] A. Durmayaz, O. Salim, B. Sahin, H. Yavuz, Optimization of thermal systems based on finite-time thermodynamics and thermoeconomics, Prog. Energy Combust. Sci. 30 (2004) 175–217, doi:10.1016/j.pecs.2003.10.003.

[39] L. Chen, H. Feng, Z. Xie, Generalized thermodynamic optimization for iron and steel production processes : theoretical exploration and application cases, Entropy 18 (2016) 353, doi:10.3390/e18100353.

[40] C.N. Markides, Low-concentration solar-power systems based on organic rankine cycles for distributed-scale applications: overview and further developments, Front. Energy Res. 3 (December) (2015) 1–16, doi:10.3389/fenrg.2015.00047.

[41] M. White, The Design and Analysis of Radial Inflow Turbines Implemented within Low Temperature Organic Rankine Cycles, City, University of London, 2015 Phd.

[42] H. Legmann, Recovery of industrial heat in the cement industry by means of the ORC process, IEEE Cement Ind. Tech. Conf. (2002) 29–35, doi:10.1109/CITCON.2002.1006482.

[43] C. Brandt, N. Schüler, M. Gaderer, J.M. Kuckelkorn, Development of a thermal oil operated waste heat exchanger within the off-gas of an electric arc furnace at steel mills, Appl. Therm. Eng. 66 (1–2) (2014) 335–345, doi:10.1016/j.applthermaleng.2014.02.003.